

**FAST SOLUTION OF CHROMATOGRAPHIC PARTICLE
AND COLUMN MODELS ON PARALLEL COMPUTERS**

E. von Lieres¹§, C. Frauen², K. Nöh³

^{1,2,3}Research Centre Jülich

Leo Brandt Strasse, Jülich, 52425, GERMANY

¹e-mail: e.von.lieres@fz-juelich.de

Abstract: Fast solution of chromatography models is crucial for parameter estimation and rational process design. Two submodels of the general rate model are chosen for assessment of parallel solution techniques. The submodels describe isolated porous particles, and chromatographic columns with non-porous particles, respectively. Numerical results prove efficiency of the parallel approach for both models, and encourage implementation of a parallel solver also for the general rate model, which describes column chromatography with porous particles.

AMS Subject Classification: 92A08

Key Words: chromatography, modeling, partial differential algebraic equations, high performance computing

1. Introduction

Ion exchange chromatography is commonly applied for protein separation in biopharmaceutical industry. Purification of pharmaceutical products typically requires several individually designed chromatographic steps. Design and optimization of these separation processes for new products are time consuming and expensive. Here, quantitative simulation of chromatographic biomolecule separation would certainly help speed up process design and cut down costs. However, chromatography models comprise various parameters whose values need to be estimated from experimental data.

Received: August 17, 2007

© 2008, Academic Publications Ltd.

§Correspondence author

Modern observation techniques, such as confocal laser scanning microscopy (CLSM), nowadays provide comprehensive data of increasing quantity and quality. Model based analysis of these data is computationally very demanding, particularly for multi-component systems, since parameter estimation involves repetitive solution of nonlinear and stiff partial differential-algebraic equation systems. Hence, fast solution of chromatography models is crucial for both rational analysis and model based design of separation processes for biomolecules.

2. Chromatography

Chromatography is often performed in columns that are packed with porous beads, as illustrated in Figure 1, involving several transport and sorption processes on different scales. Qualitative and quantitative understanding of these mechanisms as well as their interplay is crucial for the analysis and simulation of the entire separation process: Proteins are transported through the column in a buffer solution by convective flow. In the packed bed they are subject to dispersion, which is mainly caused by eddies and other flow inhomogeneities. Moreover, concentration gradients between the bulk flow and a stagnant film at the bead surfaces are leveled by film diffusion.

Inside the chromatographic beads, the molecules diffuse through pores until they are adsorbed at the pore walls, which is in ion-exchange chromatography due to electrostatic interaction. The adsorbent surfaces are initially covered with salt ions from the buffer solution in order to maintain electroneutrality. Large adsorbate molecules with complex surface charge distributions typically occupy more than one binding site and exclude additional sites from further binding by steric shielding. In dynamic sorption equilibrium, adsorbed proteins are also subject to desorption and displacement by competing species. The global separation process is strongly governed by different surface affinities, while different dispersion and diffusion rates, which correlate with molecule size, impact less on overall performance.

3. Chromatography Models

Two subsystems have been chosen for the assessment of parallel solution techniques for chromatography models: The first model, which is commonly applied for batch chromatography, describes the separation process in an isolated particle. The second model describes single-component column chromatography

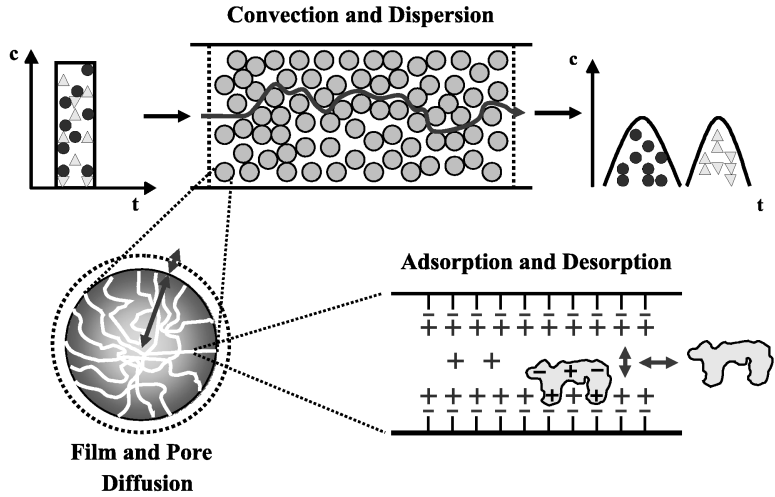


Figure 1: Transport and separation mechanisms of liquid column ion exchange chromatography

with non-porous particles.

3.1. Particle Model

The migration and competitive sorption of salt ions and proteins in a porous particle is described by a system of partial differential-algebraic equations. The steric mass action (SMA) formalism (see [1]) is applied to describe competitive sorption of salt ions (component $i = 1$) and different protein species (components $i = 2..n$): The local adsorption rate of component $i \geq 2$ is proportional to protein concentration c_i in the mobile phase, that is the pore fluid, and ν_i -fold proportional to the concentration of available counter ions \bar{q}_1 in the stationary phase, that is at the pore surface, where ν_i is the respective protein's characteristic charge. Analogously, the local desorption rate is proportional to protein concentration q_i in the stationary phase, and ν_i -fold proportional to salt concentration c_1 in the mobile phase. Proportionality factors are the component-specific adsorption and desorption constants $k_{a,i}$ and $k_{d,i}$. The concentrations c_i , q_i and \bar{q}_1 are functions of the time t and space in which, due to particle symmetry, only the radial coordinate r needs to be considered:

$$\frac{\partial q_i}{\partial t} = k_{a,i} \cdot c_i \cdot \bar{q}_1^{\nu_i} - k_{d,i} \cdot c_1^{\nu_i} \cdot q_i. \tag{1}$$

Equation (1) is valid only for components $i \geq 2$, whereas the stationary phase concentration of available counter ions \bar{q}_1 is algebraically determined by the electroneutrality condition:

$$\Lambda = \bar{q}_1 + \sum_{i=2}^n (\nu_i + \sigma_i) \cdot q_i. \quad (2)$$

Here, Λ denotes the specific surface charge and σ_i the proteins' steric factor, which quantifies the steric shielding of surface charges.

Another set of equations for components $i = 1 \dots n$ are derived from mobile phase mass balances (see [3]):

$$\frac{\partial c_i}{\partial t} + \frac{1}{\beta} \cdot \frac{\partial q_i}{\partial t} = d_i \cdot \left(\frac{\partial^2 c_i}{\partial r^2} + \frac{2}{r} \cdot \frac{\partial c_i}{\partial r} \right). \quad (3)$$

The right hand side of equation (3) describes diffusion with rate d_i in spherical coordinates. The phase ratio β on the left hand side of equation (3) accounts for different volume fractions of the mobile and stationary phase.

The model equations are supplemented by boundary conditions for the time span $0 \leq t \leq T$. Owing to symmetry, both stationary and mobile phase fluxes of components $i = 1 \dots n$ vanish at the particle center $r = 0$:

$$\frac{\partial \bar{q}_1}{\partial r}(t, 0) = 0, \quad \frac{\partial q_i}{\partial r}(t, 0) = 0, \quad \text{and} \quad \frac{\partial c_i}{\partial r}(t, 0) = 0. \quad (4)$$

The stationary phase fluxes of components $i = 1 \dots n$ also vanish at the particle boundary $r = R$:

$$\frac{\partial \bar{q}_1}{\partial r}(t, R) = 0 \quad \text{and} \quad \frac{\partial q_i}{\partial r}(t, R) = 0. \quad (5)$$

The respective mobile phase fluxes that are caused by pore and film diffusion must be equal. Here, the film diffusion is considered proportional to the difference between protein concentration $c_{b,i}$ in the surrounding bulk phase and c_i in the particle pores. Proportionality factors are the component-specific film diffusion coefficients $k_{f,i}$:

$$d_i \cdot \frac{\partial c_i}{\partial r}(t, R) = k_{f,i} \cdot (c_{b,i}(t) - c_i(t, R)). \quad (6)$$

The initial conditions are chosen such as to represent an unloaded particle, whose binding sites are saturated with salt ions in order to maintain electroneutrality at radial coordinates $0 \leq r \leq R$:

$$\bar{q}_1(0, r) = \Lambda \quad \text{and} \quad c_1(0, r) = c_1(0), \quad (7)$$

$$q_i(0, r) = 0 \quad \text{and} \quad c_i(0, r) = 0 \quad \text{for } i = 2 \dots n. \quad (8)$$

3.2. Column Model

The Langmuir formalism is applied to describe single-component sorption on column scale: The local adsorption rate is proportional to protein concentration c_f in a stagnant film that surrounds the non-porous particles, and to the availability of binding sites, which is the difference of the maximum capacity q_m and protein concentration at the surface q . Counter ions are not considered in this model and, hence, the local desorption rate is only proportional to protein concentration at the surface. Proportionality factors are the adsorption and desorption constants k_a and k_d , respectively:

$$\frac{\partial q}{\partial t} = k_a \cdot c_f \cdot (q_m - q) - k_d \cdot q. \quad (9)$$

Film mass transfer is proportional to the difference between concentration c in the bulk phase, where the molecules are subject to convection, and in the stagnant film. Proportionality factor is the film diffusion coefficient k_f . The coefficient $0 \leq \varepsilon_f \leq 1$ accounts for different volume fractions of the stationary phase and stagnant film (see Figure 2):

$$\varepsilon_f \cdot \frac{\partial c_f}{\partial t} + (1 + \varepsilon_f) \cdot \frac{\partial q}{\partial t} = k_f \cdot (c - c_f). \quad (10)$$

The balance equation for the mobile phase describes convection with flow rate ν and dispersion with rate coefficient d . The coefficient $0 \leq \varepsilon \leq 1$ denotes overall volume fraction of the mobile phase:

$$\frac{\partial c}{\partial t} + \frac{1 - \varepsilon}{\varepsilon} \cdot \left(\varepsilon_f \cdot \frac{\partial c_f}{\partial t} + (1 - \varepsilon_f) \cdot \frac{\partial q}{\partial t} \right) = -\nu \cdot \frac{\partial c}{\partial z} + d \cdot \frac{\partial^2 c}{\partial z^2}. \quad (11)$$

Danckwerts boundary conditions (see [2]) are applied at the inlet ($z = 0$) and outlet ($z = L$) of the column for the time span $0 \leq t \leq T$:

$$\frac{\partial c}{\partial z}(t, L) = 0 \quad \text{and} \quad \nu \cdot c_{in}(t) = \nu \cdot c(t, 0) - d \cdot \frac{\partial c}{\partial z}(t, 0). \quad (12)$$

The initial conditions are chosen to represent an unloaded column over the entire length $0 \leq z \leq L$:

$$c(0, z) = 0, \quad c_f(0, z) = 0 \quad \text{and} \quad q(0, z) = 0. \quad (13)$$

Figure 2 illustrates modeling of the columns subdivision into mobile phase, stagnant film and stationary phase, as well as the respective state variables and model parameters.

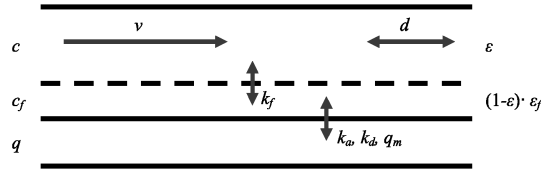


Figure 2: Phase ratios, transport and rate constants of the column model

4. Parallel Solution

Both models are discretized in the spatial variable, following the method of lines, see [5]: The corresponding partial derivatives are replaced by suitable differential quotients on equidistant meshes with n knots. The resulting systems are stiff due to diffusion or dispersion, respectively. In order to avoid numerical instabilities, the first derivatives in the column model are approximated with the WENO method (weighted essentially non oscillatory, see [6]): The weighted sum of several differential quotients of lower order is taken instead of one differential quotient of high order. The resulting large systems of ordinary differential-algebraic equations are solved with the implicit differential-algebraic solver *IDA* (version 2.3.0) from the suite of nonlinear differential algebraic equation solvers (*SUNDIALS*, Lawrence Livermore National Laboratory, see [4]).

The solver *IDA* is implemented in ANSI C and uses a linear multistep method, the backward differentiation formula (BDF), with stepwidth control and variable order. This requires solving a nonlinear algebraic equation system for each time step, and Newton iteration yields a series of linear algebraic equation systems. *IDA* provides parallel routines for solving these systems with the scaled preconditioned general minimal residual method (SPGMR). A parallel band block diagonal preconditioner module utilizes symbolically computed Jacobian matrices. The individual processes communicate via message parsing interface (MPI) to exchange state information on boundary knots.

5. Results and Discussion

Tables 1 and 2 show typical parameter sets for which the particle and column models are solved. In the particle model, all concentrations $c_{b,i}$ at the boundary $r = R$ are set to constant values for $i = 1..n$. In the column model, a pulse function of length t_0 is chosen as concentration profile c_{in} at the inlet.

$r = 45 \mu m$	$c_{p,2} = 1.43 \cdot 10^{-1} mM$	$c_{p,3} = 1.43 \cdot 10^{-3} mM$
$\varepsilon_p = 0.75$	$k_2 = 3.55 \cdot 10^{-2}$	$k_3 = 6.11 \cdot 10^{-1}$
$\Lambda = 1200 mM$	$\nu_2 = 4.7$	$\nu_3 = 3.93$
$c_1 = 44.5 mM$	$\sigma_2 = 11.83$	$\sigma_3 = 11.83$
$d_1 = 7.0 \cdot 10^{-10} m^2/s$	$d_2 = 4.0 \cdot 10^{-11} m^2/s$	$d_3 = 4.0 \cdot 10^{-11} m^2/s$

Table 1: Typical parameter set for the particle model

$L = 1.3 m$	$q_m = 1.58 \cdot 10^{-7} M$
$\varepsilon = 0.7$	$\nu = 3 \cdot 10^{-2} m/s$
$\varepsilon_f = 0.1$	$d = 1 \cdot 10^{-5} m^2/s$
$k_a = 2.9 \cdot 10^6$	$t_0 = 30 s$
$k_d = 0.58$	$T = 100 s$
$k_f = 10$	$c_{in} = 1 \cdot 10^{-6} M \quad (0 \leq t \leq t_0)$

Table 2: Typical parameter set for the column model

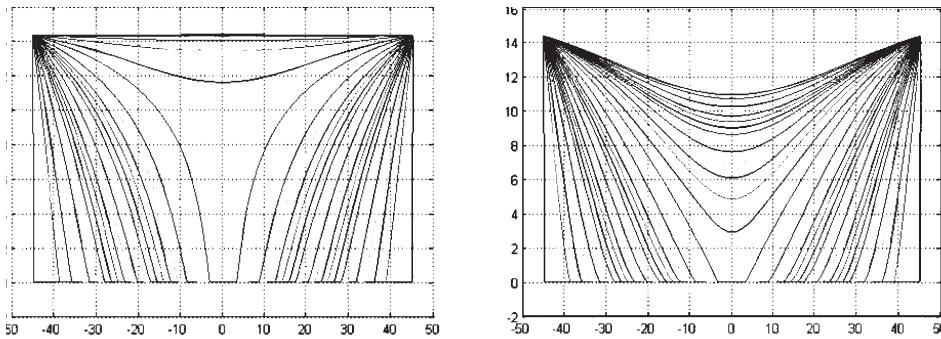
Figure 3: Mobile phase concentration c_i of components $i = 2$ and $i = 3$ over radial position r at equidistantly progressing times t

Figure 3 shows simulation results for the particle model. Both protein species migrate to the center of the particle; however, global equilibrium is reached significantly earlier by the second component, due to competitive surface interaction. Figure 4 shows simulation results for the column model. The perfect sharpness of the imposed pulse is slightly softened at the inlet due to Danckwerts boundary condition. The pulse then deteriorates over column length into a concentration profile with decreasing sharpness, and increasing width and retardation time.

Tables 3 and 4 show computation times for varied numbers of knots and

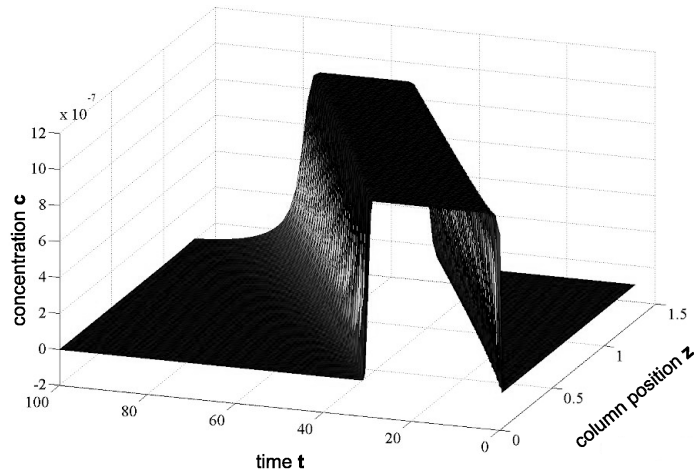


Figure 4: Mobile phase concentration over column position and time

Knots	Runtime
128	39 s
256	199 s
512	1018 s
1024	6410 s
2048	40221 s

Processors	Runtime
2	6410 s
4	2231 s
8	842 s
16	463 s
32	346 s

Table 3: Runtime of the parallel particle code on two processors for varied discretizations, and for 1024 spatial knots and varied processor numbers.

processors. All calculations were performed in Jülich on the supercomputer JUMP. The absolute computation times might be decreased by more efficient calculation of the right hand side and the Jacobian matrix of the discretized differential equation systems; however, in this study we focus on the relative speed gain.

The results prove that numerical solution of chromatography models can be sped up at least by an order of magnitude on both particle and column scale. This is particularly interesting since parallel computing is today no longer limited to supercomputers. Currently there is a clear trend towards multiprocessor and multicore technology also for standard personal computers, which cannot

Knots	Runtime	Processors	Runtime
128	1.4 s	2	93.2 s
256	5.4 s	4	26.3 s
512	23.2 s	8	9.2 s
1024	93.2 s	16	4.2 s

Table 4: Runtime of the parallel column code on two processors for varied discretizations, and for 1024 spatial knots and varied processor numbers.

be economically utilized without suitable parallel algorithms. The results encourage implementation of a parallel solver for the general rate model that combines the features of both assessed submodels.

References

- [1] C.A. Brooks, S.M. Cramer, Steric mass-action ion exchange: Displacement profiles and induced salt gradients, *AIChE Journal*, **38** (1992), 1969-1978.
- [2] P.V. Danckwerts, Continuous flow systems: Distribution of residence times, *Chemical Engineering Science*, **2** (1953), 1-13.
- [3] S.R. Gallant, Modeling ion-exchange adsorption of proteins in a spherical particle, *Journal of Chromatography A*, **1028** (2004), 189-195.
- [4] A.C. Hindmarsh, R. Serban, User documentation for *IDA v2.3.0.*, *LLNL Report UCRL-SM-208112* (2005).
- [5] W.E. Schiesser, *The Numerical Method of Lines*, Academic Press, New York (1991).
- [6] C.-W. Shu, Essentially non-oscillatory and weighted essentially non-oscillatory schemes for hyperbolic conservation laws, *ICASE Report*, No. 97-65, NASA-CR/97-206253 (1997).

